

3 UNVEILING THE NATURE OF THE UNIDENTIFIED γ -RAY SOURCES VI:
4 γ -RAY BLAZAR CANDIDATES IN THE WISH SURVEY AND THEIR RADIO PROPERTIES

5 M. NORI^{1,2}, M. GIROLETTI¹, F. MASSARO³, R. D'ABRUSCO⁴, A. PAGGI⁴, G. TOSTI^{5,6}
6 *version November 5, 2013*

7 ABSTRACT

8 According to the second *Fermi* LAT Catalog (2FGL), about one third of the γ -ray sources listed
9 has no assigned counterpart at lower energies. Many statistical methods have been developed to find
10 the proper counterpart for these sources. We explore the sky-area covered at low radio frequency by
11 Westerbork in the Southern Hemisphere (WISH) survey to search for blazar-like candidates among
12 the unidentified γ -ray sources listed in the 2FGL (UGSs). Combining the WISH and the NVSS radio
13 surveys within the positional uncertainty of the 2FGL UGSs, we select as γ -ray blazar candidates
14 the radio sources characterized by flat radio spectrum between 352 and 1400 MHz. We find 14
15 new gamma-ray blazar candidates, that could be associated to 8 UGSs and we also discuss on their
16 spectral properties at low radio frequencies. We compare the radio flux density distribution of the
17 low-frequency selected γ -ray blazar candidates with those of the blazar population associated with
18 other methods finding significant differences. Finally, we discuss the results of this association method
19 and its possible applicability to other regions of the sky and future radio surveys.

20 *Subject headings:* galaxies: active - galaxies: BL Lacertae objects - radiation mechanisms: non-thermal

21 1. INTRODUCTION

22 In the last decades, γ -ray astrophysics has undergone
23 some stunning improvements due to the great efforts and
24 achievements in the high energy technologies. Up to
25 date, the most recent and most accurate γ -ray source
26 catalog is the *Fermi* Large Area Telescope (LAT) Sec-
27 ond Source Catalog (2FGL, Nolan et al. 2012), com-
28 piled on the data provided by the *Fermi* γ -ray Space
29 Telescope on 24 months of data. Thanks to its silicon
30 strip pair production and modern analysis processes, the
31 LAT has drastically reduced the positional error of the
32 sources with respect to previous studies, like those per-
33 formed by the Energetic Gamma-Ray Experiment Tele-
34 scope (EGRET) on board the Compton Gamma-Ray Ob-
35 servatory (Hartman et al. 1999).

36 However, the γ -ray positional uncertainty remains sig-
37 nificantly larger in comparison to the other surveys at
38 lower energies, making the multifrequency association
39 challenging. Several association methods were proposed
40 to match the γ -ray sources detected with source catalogs
41 at lower frequencies (Paggi et al. 2013) (Masetti et al.
42 2013), to give a proper counterpart to each and every
43 source. In the 2FGL, there are 575 sources, out of 1873,
44 whose physical nature is still unknown. Regarding the
45 *Fermi* sources we do know the nature of, blazars are the
largest known population representing more than 80%.

¹ INAF Istituto di Radioastronomia, via Gobetti 101, 40129, Bologna, Italy

² Dipartimento di Fisica e Astronomia, Università di Bologna, viale Berti Pichat 6/2, 40127 Bologna, Italy

³ SLAC National Laboratory and Kavli Institute for Particle Astrophysics and Cosmology, 2575 Sand Hill Road, Menlo Park, CA 94025, USA

⁴ Harvard - Smithsonian Astrophysical Observatory, 60 Garden Street, Cambridge, MA 02138, USA

⁵ Dipartimento di Fisica, Università degli Studi di Perugia, 06123 Perugia, Italy

⁶ Istituto Nazionale di Fisica Nucleare, Sezione di Perugia, 06123 Perugia, Italy

46 It is, therefore, fair to presume that a significant fraction
47 of the unidentified γ -ray sources (UGSs) can be unrec-
48 ognized blazar-like sources. Finding them is the aim of
49 our work.

50 Blazars are compact radio sources with a flat (i.e.,
51 spectral index $\alpha < 0.5$, where $S_\nu \sim \nu^{-\alpha}$) radio spectrum
52 that steepens towards the infrared-optical bands; their
53 overall spectral energy distribution shows two broadband
54 components: the low energy one peaking in the IR-to-X
55 ray frequency range, while the high energy one extends
56 up to the MeV-to-TeV range. Their emission features
57 high and variable polarization, apparent superluminal
58 motions of radio jet components and high apparent lumi-
59 nosity, coupled with rapid flux variability over the whole
60 electromagnetic spectrum. Blazars come into two classes:
61 flat-spectrum radio quasars and BL Lac objects, which
62 we label here as BZQs and BZBs respectively, follow-
63 ing ROMA-BZCAT (Massaro et al. 2009) nomenclature.
64 Blazar emission is interpreted as radio loud active galax-
65 ies, with one of the relativistic jets emerging from the
66 super massive black hole in the galaxy nucleus pointing
67 almost directly to the observer (Giommi et al. 2012).

68 This paper is the latest part of a series that focus on the
69 nature of UGSs, consisting in: D'Abrusco et al. (2013)
70 (hereafter Paper I), which look into the peculiar IR colors
71 of blazars, in order to recognize a blazar-like sources as
72 UGSs counterparts as described in Massaro et al. (2013a,
73 Paper II); Massaro et al. (2013b, Paper III) adds another
74 feature for the search of blazar-like sources focusing on
75 the low-frequency radio feature of blazars; Paggi et al.
76 (2013, Paper IV) involve the X-ray emission as a distinc-
77 tive feature and Massaro et al. (2013c, Paper V) propose
78 a renewed IR approach, based on a 2-dimensional ker-
79 nel density estimation (KDE) technique, all for the same
80 purpose.

81 In this work, we apply the method proposed in Pa-
82 per III to search for blazar-like sources within the γ -ray
83 positional uncertainty of the UGSs listed in the 2FGL

and to select candidates as counterpart among them. This method is based on a multifrequency procedure, relying primarily on the flatness of the radio spectrum. The innovative point in this method is that it is based on low-frequency (i.e., < 1 GHz) measurements, which is unprecedented in the investigation of the blazar emission and their association with UGSs. In Paper III, we combined the observations at 325 MHz performed in the Westerbork Northern Sky Survey (WENSS) at 325 MHz with those of the NRAO Very Large Array Sky Survey (NVSS) at 1.4 GHz. In this work, we apply the same approach to the region covered by the twin survey of WENSS in the southern sky: the Westerbork in the Southern Hemisphere (WISH, De Breuck et al. 2002). Thanks to the combined results of this new search and of Paper III, we build a reasonably sized population of new low-frequency selected blazar candidates. We study the spectral properties of individual candidates and explore the flux density distribution of the whole sample in comparison to the γ -ray blazars already listed in the 2nd *Fermi* LAT Catalog of Active Galactic Nuclei (2LAC, Ackermann et al. 2011b). We further refine our search by looking for IR, optical, UV and X-ray counterpart within the catalogs available.

The paper is organized as follows: in Sect. 2 we describe our method; in Sect. 3 we report and characterize our list of candidates; in Sect. 4 we discuss the spectral properties of all the sources found with the low-frequency method and give some outlook on the expectations from new instruments in the low frequency radio regime.

2. METHOD

2.1. Blazar features in low frequency radio band

The features of blazars (in particular γ -ray emitting blazars) in this electromagnetic spectrum region are discussed in Paper III; we briefly summarise those results here for the sake of clarity.

Based on the cross correlation between the 2FGL catalog, the ROMA-BZCAT v4.1 (the most comprehensive blazar catalogue up to now), and the WENSS, we defined one sample labeled as Low Radio frequency (LB) and a subsample labeled Low radio frequency γ -ray Blazar (LGB). Since ROMA-BZCAT catalog is based on NVSS survey, we easily computed the low frequency radio spectral index as:

$$\alpha_{\nu}^{1400} = \log\left(\frac{S_{1400}}{S_{\nu}}\right) / \log\left(\frac{\nu}{1400}\right) \quad (1)$$

where ν is the low radio frequency in consideration measured in MHz (i.e., 325 for WENSS and 352 for WISH) and both flux densities are measured in mJy.

The indices of about 80% of the sources from both LB and LGB sample are smaller than 0.5 and 99% have indices below 1.0 (Massaro et al. 2013b). The flatness of the radio spectrum can be seen as a consequence of the dominance, also at low radio frequencies, of the inner jet departing from the core on the emission radiated by the larger structures of the blazar.

In particular for the γ -ray blazar sample, we consider *A class* candidates the radio sources characterized by $-1.0 \leq \alpha_{352}^{1400} \leq 0.55$; *B class* those with $0.55 \leq \alpha_{352}^{1400} \leq 0.65$, within the errors. These two classes have been defined to represent respectively the 80% (*A class*) and 90%

(*B class*) upper limits of γ -ray blazar radio spectral indices. In fact, the flatness of radio spectrum above 1 GHz is indeed a well known feature and was already adopted to select γ -ray blazar candidates in the past (Healey et al. 2008). However the low-frequency radio observations allow us to confirm this flatness down to 325 MHz.

2.2. The WISH survey

The WISH survey is the natural extension of the WENSS survey to 1.60 sr of the southern sky and it was performed at 352 MHz between 1996 and 1999. It covers the area between $-9^{\circ} < \text{Dec} < -26^{\circ}$ to a limiting flux density of ~ 18 mJy (5σ), the same as the WENSS. Due to the low elevation of the observations, the survey has a lower resolution in declination than in right ascension ($54'' \times 54'' \times \csc(\delta)$). Besides this, the WISH shares with the WENSS the same features upon which this method was calibrated, except for a negligible difference in frequency ($\Delta\nu = 27$ Hz). For this reason, we are confident to apply the same association procedure used on WENSS.

2.3. Association procedure

Starting from each UGS in the WISH footprint, we search for low frequency sources in a circular region of radius equal to the major semi axis of the 95% confidence level positional uncertainty ellipse of the UGSs itself. We only consider WISH sources classified as single component sources. For each WISH source found, we look for a NVSS source in a circular region of radius equal to $8.5''$ and we then calculate the radio spectral index α_{352}^{1400} .

In addition, we made local maps of the search regions for each UGS, overlaying on the WISH background the contours of NVSS map, the *Fermi* positional uncertainty ellipse, and any possible blazar-like *WISE* detection up to $3.3''$ from the NVSS match position. This gave us, in addition to a qualitative comparison of the relative position of various possible candidates and the UGS, a clue about their eventual non-blazar nature if complex structures are visible. The angular separation between a candidate and the center of the *Fermi* ellipse might be taken in account in case of multiple matches, preferring the nearest source rather than others.

2.4. Multi-frequency data

Finally, we looked for additional multifrequency data for our new blazar candidates and those found in Paper III. In particular, we searched for matches with the Australia Telescope 20 GHz survey (AT20G, Murphy et al. 2010) for the WISH candidates, and in the Green Bank 4.85 GHz northern sky survey (GB6, Gregory et al. 1996) for the WENSS candidates. The AT20G survey, performed between 2005 and 2006, contains sources with $S_{20.0} \geq 40$ mJy; the GB6, performed between 1986 and 1987 from the NRAO seven-beam receiver, takes in account sources with $S_{4.85} \geq 18$ mJy. For these surveys, source association is automatically provided by NED. We also refer to Paggi et al. (2013) for the analysis of X emission, performed by the Swift X-ray Telescope.

For our own association method between WISH and NVSS and between NVSS and WISE, the search radius (of $8.5''$, and $3.3''$, respectively) are based upon a statistical basis, as described in Paper III.

3. RESULTS

3.1. UGSs in the WISH footprint

According to the 2FGL catalog, the complete list of UGSs counts 575 sources. We discard all the sources that feature a ‘c’ analysis flag to rule out the potentially confused undetected sources due to the strong interstellar emission (Nolan et al. 2012). The resulting list of UGSs on the WISH footprint counts 27 γ -ray sources. Of these, 17 have at least a WISH and NVSS match. We report the list of these 17 UGSs in Table 1. For each source, we list the 2FGL name (Col. 1), the list of possible radio counterparts in the WISH (Col. 2) and NVSS (Col. 3) surveys, the corresponding flux density at 352 MHz (Col. 4) and 1400 MHz (Col. 5), the presence in the *WISE* catalog (Col. 6), the low frequency radio spectral index (Col. 7) and the relative classification.

Eight out of 17 of these UGSs present a unique match in the radio surveys while the other 9 present multiple correspondences. The total number of simultaneous UGSs-WISH-NVSS matches is 31. Nine of these matches have a radio spectral index $\alpha_{325}^{1400} < 0.55$ and are considered *class A* candidates while 5 have $0.55 < \alpha_{325}^{1400} < 0.65$ and are considered *class B* candidates. We show two sample fields in Fig. 1.

Fourteen out of the 31 matches in the WISH footprint feature a *WISE* detection in at least two IR bands; six out of 14 *A* and *B* candidates feature *WISE* detection. However, we do not consider the *WISE* detection to be necessary for selection. Flat spectrum radio quasars at high-redshift or high synchrotron peaked BZBs could be too faint in the IR and to be detected in one or more *WISE* bands; moreover, the relative astrometry of the WISH and NVSS could not be as good in this region (Massaro et al. 2013c).

All considered, we propose 14 new blazar-like candidates (i.e., *A* and *B* class candidates) as counterpart for 8 UGSs. In particular, we increase the number of *class A* candidates from the low frequency method applied to the WENSS and the WISH footprints to 29.

3.2. Multiwavelength observations and radio flatness of low-frequency selected blazar candidates

In this work and in Paper III, we evaluate the flatness of the radio spectrum according to Exp. 1 on the basis of just two non-simultaneous flux density measurements, one at 1.4 GHz (NVSS) and the other at low frequency (352 MHz for the WISH or 325 MHz for the WENSS). For this reason, it is important to find other radio flux density data to better investigate the spectral and variability properties of the new candidates. We looked for other radio surveys in literature performed in the WENSS and WISH footprint; we consider here all the candidates found both in Paper III and in the present work.

In the WENSS footprint, we found that 6 *A class* and 2 *B class* candidates are listed in the GB6 survey. We report in Table 2 the list of these sources along with the radio spectral index, obtained with a weighted linear regression on the three frequencies. For all these sources, the 5 GHz flux density is in good agreement with the extrapolation of the low frequency spectrum, confirming that the radio spectrum is flat and flux density variability is not dramatic, if any. A sample spectrum is shown in

Fig. 2 (left panel).

In the WISH footprint, we find that one *A class* (WNB 1251.8–2148, alias NVSS 125429–220419), but no *B class* candidates, is also listed in the AT20G. Data and radio spectral index regression are reported in Table 3 (see also Fig. 2, right panel). In this case, the extrapolation of the low frequency power law clearly fails to match the high frequency data, suggesting prominent variability or a rather complex spectral shape, with a strongly inverted component above a few GHz; either way, the source behavior is consistent with being a γ -ray blazar candidate.

4. DISCUSSION AND CONCLUSIONS

4.1. Comparison with Paper III

As the *Fermi*-LAT γ -ray observations of the sky continue, the task of finding a clear counterpart to all the detected sources becomes increasingly challenging, mostly due to the large positional uncertainty of the faintest sources. Since a strong connection between gamma-ray and radio emission has been clearly demonstrated (Ackermann et al. 2011a; Ghirlanda et al. 2010; Mahony et al. 2010), it is natural to exploit radio surveys for finding new associations. Our goal is to apply the method recently proposed in Paper III to an additional sky area, aiming to reduce the amount of these UGSs (amounting to $\sim 30\%$ of the total in the 2FGL). The method is based on a study of the low-frequency spectral properties of blazars (and γ -ray blazars in particular).

In the present paper, we applied this method, that was elaborated starting from WENSS data, to the WISH sky region. The WENSS and WISH surveys, both performed by the Westerbork Synthesis Radio Telescope (WSRT) telescope in the 1990s, have similar frequency range of observation (i.e. 325 MHz and 352 MHz respectively) and same limiting flux density of ~ 18 mJy (5σ). They share also the bandwidth synthesis mosaicing technique, used to combine 8 different bands of 5 MHz. The resolution is one of the main difference between the two surveys, because due to the low elevation of the observation for WISH, resolution in declination is poorer than for WENSS by a factor $\sim 2\times$ on average.

However, this difference would mainly affect the spatial association and not the parameters on which the counterpart is chosen. Since spatial association is calibrated on a higher resolution survey like WENSS, applying it to the WISH region and catalog results in a more conservative approach. The fact we found almost the same ratio (i.e. ~ 1.8) of radio sources per UGS in both WENSS and WISH (58 WENSS candidates for 32 UGSs and 31 WISH candidates for 17 UGSs) proves that, on average, spatial association is not compromised.

Similarly, the poorer resolution in declination can not be blamed for any impact on the quality of the proposed counterparts, given the similar rate of γ -ray blazar-like counterparts proposed in the two survey application. In fact, in Paper III we have 23 proposed new γ -ray blazars out of 65 UGSs in WENSS region (i.e. 35%) and 8 out of 27 in WISH region (i.e. 30%)⁷.

⁷ The small discrepancy can be explained, in addition to simple statistics, also on the grounds of the slightly different starting list, since in Paper III we considered only γ -ray sources without *any*

4.2. Comparison with other methods

Other methods have been suggested to recognize low-energy counterparts to UGSs, or at least to provide a statistically significant classification of these sources. For instance, Ackermann et al. (2012) have developed a statistical approach to classify UGSs in the first catalog of *Fermi* sources (1FGL, Abdo et al. 2010). Six of the 2FGL UGSs in the WISH footprint are associated to 1FGL sources analyzed by Ackermann et al. (2012), 5 of which are AGN-like and one of which is pulsar-like. Within the former sample, there are two sources for which we propose a candidate blazar counterpart on the basis of the low frequency spectrum: 2FGL J2017.5–1618 and 2FGL J2358.4–1811. Interestingly, for the single UGS for which Ackermann et al. (2012) propose a pulsar classification (2FGL J1544.5–1126), our methods finds a WENSS-NVSS match with quite steep spectral index ($\alpha = 0.74 \pm 0.03$), rejecting a blazar scenario.

We further compared our results with the proposed associations found in the other papers of this series. In Figure 3 we show the comparison between the distribution in the IR $[3.4] - [4.6] - [12] \mu\text{m}$ color-color plane provided by *WISE* for the γ -ray emitting blazars and the sources selected in this work. The overall distribution of the whole set of the simultaneous WISH-NVSS matches (black, red and green dots) is quite more scattered than the γ -ray blazar population (orange dots). However, when we only consider the low-frequency selected blazar candidates, all the most prominent outliers are excluded and the remaining 6 sources (black and red dots) are in much better agreement with the IR colors of γ -ray blazars. In two cases, the A-class candidates NVSS 120900–231335 and NVSS 222830–163643, the agreement is perfect. For the latter source, associated to 2FGL J2228.6–1633, our method also provides the same candidate selected on the basis of the kernel density estimator technique to IR colors of WISE counterparts applied to X-ray (Paggi et al. 2013) and radio (Massaro et al. 2013c) data.

4.3. Radio flux density analysis

The γ -ray blazar candidates selected in this work and in Paper III have by selection the same radio spectral properties of confirmed ROMA-BZCAT blazars and of 2FGL blazar associations. It is natural to wonder why these sources have not been detected and eventually associated, e.g. in the second catalog of AGNs detected by *Fermi* (Ackermann et al. 2011b). The sources could have been excluded from the 2LAC because they do not formally pass the threshold for being considered high confidence associations (a test that does not take into account the spectral index); typically, this could happen for low flux density radio sources, which have a larger spatial density. It is thus likely that, side-by-side with a general similarity to the already known blazars, our new candidates have also some peculiarity.

For this reason, we show in Fig. 4 the distribution of radio flux density at 1.4 GHz for all the blazars in the 2LAC and for the candidates selected here and in Paper III. The two distributions are clearly different, as confirmed by a K-S test which yields a probability of

analysis flag, while here we excluded only the sources with the γ -ray analysis flag in the 2FGL (Nolan et al. 2012).

2.7×10^{-15} of being obtained from the same population. In particular, the 2LAC blazar flux density distribution is shifted to much larger values. This strongly suggests that our method is very efficient in selecting faint blazars. These sources are potentially of great interest: if they are of the BZB type, it could mean that they could be of the extreme and elusive class of ultra-high synchrotron peaked sources; one prominent example could be WNB 2225.8–1652, which has an inverted radio low frequency spectral index of $\alpha = -0.19 \pm 0.10$ and is our proposed counterpart for the UGS 2FGL J2228.6–1633, characterized by a γ -ray spectrum as hard as $\Gamma = 2.07 \pm 0.16$. On the other hand, some of our candidates could also be faint BZQ, and in this case their low flux density could stem from their high redshift (Massaro et al. 2013b, like WN 1500.0+4815 with estimate redshift of 2.78, see), which would also make them of valuable scientific interest.

4.4. Summary and outlook

We have searched the 27 UGS in the 1.6 sr footprint of the WISH survey, following the methods described in Paper III and based on the flat spectrum at low frequency characteristic of blazars. We have found blazar-like associations for 8 UGSs, that together with the 23 sources selected in the WENSS footprint with the same method provides a blazar association for a sample of 30 new γ -ray blazar candidates. This sample extends the distribution of the radio flux density of γ -ray blazars to lower values, allowing us to study otherwise elusive AGNs.

The application of our method thus shows promising results in terms of numbers of counterparts proposed and their physical features. In particular, the possibilities in particular regarding the use of low frequency radio data to find UGSs counterparts are even more important in the light of the imminent start of different studies in this emission range, like the LOw Frequency ARray (LOFAR, van Haarlem et al. 2013), the Murchison Widefield Array (MWA, Tingay et al. 2013), the Long Wavelength Array (LWA, Ellingson et al. 2009), and eventually the Square Kilometer Array (SKA, e.g. Dewdney et al. 2010). These facilities will allow to extend our method using even deeper and simultaneous dataset, while dedicated targeting of the candidates with optical spectroscopy and VLBI observations will confirm the nature of the proposed counterparts.

M. Giroletti acknowledges financial contribution from grant PRIN-INAF-2011. The work is supported by the NASA grants NNX12AO97G and NNX13AP20G. R. D’Abrusco gratefully acknowledges the financial support of the US Virtual Astronomical Observatory, which is sponsored by the National Science Foundation and the National Aeronautics and Space Administration. The work by G. Tosti is supported by the ASI-INAF contract I/005/12/0. This research has made use of data obtained from the High Energy Astrophysics Science Archive Research Center (HEASARC) provided by NASA’s Goddard Space Flight Center; the SIMBAD database operated at CDS, Strasbourg, France; the NASA/IPAC Extragalactic Database (NED) operated by the Jet Propulsion Laboratory, California Institute of Technology, under contract with the National Aeronautics and Space

Administration. Part of this work is based on the NVSS (NRAO VLA Sky Survey); The National Radio Astronomy Observatory is operated by Associated Universities, Inc., under contract with the National Science Foundation. This publication makes use of data products from the Wide-field Infrared Survey Explorer, which is a joint project of the University of California, Los Angeles, and the Jet Propulsion Laboratory/California Institute of Technology, funded by the National Aeronautics and Space Administration.

REFERENCES

- Abdo, A. A., Ackermann, M., Ajello, M., et al. 2010, *ApJS*, 188, 405
- Ackermann, M., Ajello, M., Allafort, A., et al. 2011a, *ApJ*, 741, 30
- Ackermann, M., Ajello, M., Allafort, A., et al. 2011b, *ApJ*, 743, 171
- Ackermann, M., Ajello, M., Allafort, A., et al. 2012, *ApJ*, 753, 83
- D’Abrusco, R., Massaro, F., Ajello, M., Grindlay, J. E., Smith, H. A., & Tosti, G. 2012, *ApJ*, 748, 68
- D’Abrusco, R., Massaro, F., Paggi, A., Masetti, N., Tosti, G., Giroletti, M., & Smith, H. A. 2013, *ApJS*, 206, 12
- De Breuck, C., Tang, Y., de Bruyn, A. G., Rottgering, H., & van Breugel, W. 2002, *yCat*, 8069
- Dewdney, P., et al. 2010, SKA Memo # 130, SKA Phase 1: Preliminary System Description
- Ellingson, S. W., Clarke, T. E., Cohen, A., et al. 2009, *IEEE Proceedings*, 97, 1421
- Ghirlanda, G., Ghisellini, G., Tavecchio, F., & Foschini, L. 2010, *MNRAS*, 407, 791
- Giommi, P., Polenta, G., Lhteenmki, A., et al. 2012, *A&A*, 541, 160
- Gregory, P. C., Scott, W. K., Douglas, K., et al. 1996, *ApJS*, 103, 427
- Hartman, R. C., Bertsch, D. L., Bloom, S. D., et al. 1999, *ApJS*, 123, 79
- Healey, S. E., Romani R. W., Cotter G., et al. 2008, *ApJS*, 175, 97
- Mahony, E. K., Sadler, E. M., Murphy, T., Ekers, R. D., Edwards, P. G., & Massardi, M. 2010, *ApJ*, 718, 587
- Masetti, N., Sbarufatti, B., Parisi, P., et al. 2013, submitted, arXiv, arXiv:1310.1916
- Massaro, E., Giommi, P., Leto, C., Marchegiani, P., Maselli, A., Perri, M., Piranomonte, S., & Sclavi, S. 2009, *A&A*, 495, 691
- Massaro, F., D’Abrusco, R., Tosti, G., et al. 2012, *ApJ*, 750, 138
- Massaro, F., D’Abrusco, R., Paggi, A., Masetti, N., Giroletti, M., Tosti, G., Smith, H. A., & Funk, S. 2013a, *ApJS*, 206, 13
- Massaro, F., D’Abrusco, R., Giroletti, M., Paggi, A., Masetti, N., Tosti, G., Nori, M., & Funk, S. 2013b, *ApJS*, 207, 4 (Paper III)
- Massaro, F., D’Abrusco, R., Paggi, A., et al. 2013c, *ApJ*, submitted
- Murphy, T., Sadler, E. M., Ekers, R. D., et al. 2010, *MNRAS*, 402, 2403
- Nolan, P. L., Abdo, A. A., Ackermann, M., et al. 2012, *ApJS*, 199, 31
- Paggi, A., Massaro, F., D’Abrusco, R., Smith, H. A., Masetti, N., Giroletti, M., Tosti, G., & Funk, S. 2013, *ApJ*, submitted
- Tingay, S. J., Goebel, R., Bowman, J. D., et al. 2013, *PASA*, 30, 7
- van Haarlem, M. P., Wise, M. W., Gunst, A. W., et al. 2013, arXiv, arXiv:1305.3550

APPENDIX

Notes on individual UGSs

Below, we report a brief analysis of the results regarding each individual UGSs of the 17 listed in Table 1.

- *2FGL J0340.7–2421* Both radio sources in this search region have an IR detection by *WISE*. Our method selects WN 0338.4–2436 as a blazar candidate due to its flatter (*class A*) spectral index; this source has also a larger flux density.
- *2FGL J0600.8–1949* There are three radio sources: WN 0558.8–1950 results the best candidate among the other since it is nearest to the γ -ray position and it has blazar-like IR colors, flatter spectrum, and larger flux density; however, the radio spectrum is steeper than 0.65 so we can not formally classify it as a blazar
- *2FGL J1059.9–2051* Both sources in the search region have a quite steep radio spectral index and large flux density but are detected in the IR by *WISE*.
- *2FGL J1208.6–2257* WN 1206.4–2256 is the best counterpart among the other candidates because of its flat (*class A*) spectral index and *WISE* blazar-like detection
- *2FGL J1254.2–2203* WNB 1251.8–2148 has intermediate spectral index and is proposed as a *class A* blazar candidate. It is to be noted that a second nearby 1.4 GHz source (NVSS 125422-220413, see fig. 1, right panel) is not present in the WISH survey, suggesting a flatter spectral index; this source could also be a blazar-like candidate, and a partial contributor to the γ -ray emission in this region.
- *2FGL J1458.5–2121* The only candidate has the IR features of a blazar-like source but a too steep spectral index; moreover, just outside the search region lies a much brighter source that could be the real counterpart for the UGS.
- *2FGL J1544.5–1126* The only candidate has a too steep radio spectrum and no proper *WISE* match, so it is not a likely blazar candidate. Indeed, this UGS was already detected in the 1FGL and the statistical method of Ackermann et al. (2012) suggested that it should be classified as a pulsar.
- *2FGL J1624.2–2124* Four radio sources are present within the γ -ray error radius, all with *A* or *B class* spectral index, and one with a *WISE* detection. The most promising candidates are WNB 1620.7–2120 (flattest α) and WNB 1621.1–2119 (largest flux density and presence of IR emission).
- *2FGL J1631.0–1050* None of the three radio sources within the search region has a flat spectral index; WN 1628.7–1037 has blazar-like IR colors.

- 530 • *2FGL J1646.7–1333* WN 1644.0–1323, even presenting a *WISE* detection and typical blazar-like X emission
531 (Paggi et al. 2013), has a too steep radio spectral index to be taken in account as a blazar-like counterpart.
- 532 • *2FGL J1913.8–1237* According to our method, none of the radio sources in this region can be considered a good
533 blazar candidate.
- 534 • *2FGL J2009.2–1505* The only radio source, even featuring blazar-like X emission (Paggi et al. 2013), has a
535 somewhat too steep spectral index for being considered a blazar-like source, and it also lacks of a *WISE* detection.
- 536 • *2FGL J2017.5–1618* WNB 2014.9–1627 is a *class A* blazar candidate, even if it would not be selected as such
537 on the basis of the IR emission. Ackermann et al. (2012) also classify this UGS as a likely AGN.
- 538 • *2FGL J2031.4–1842* Both sources in the search region have a *class B* radio spectral index; the most likely blazar
539 candidate is WNB 2027.8–1900, which is brighter and detected in the IR.
- 540 • *2FGL J2124.0–1513* The only radio source has a too steep spectral index for being selected as a blazar-like
541 source, and it also lacks of a *WISE* detection.
- 542 • *2FGL J2228.6–1633* The inverted spectral index of WNB 2225.8–1652, its blazar-like *WISE* colors and X
543 emission (Paggi et al. 2013) make this source a highly reliable blazar candidate and counterpart for the UGS.
- 544 • *2FGL J2358.4–1811* WNB 2355.7–1833 has a radio spectral index just above our *B class* threshold and a
545 *WISE* detection. This makes it a suitable, yet not formal, blazar-like counterpart, in agreement with the AGN
546 classification proposed for this UGS by Ackermann et al. (2012)

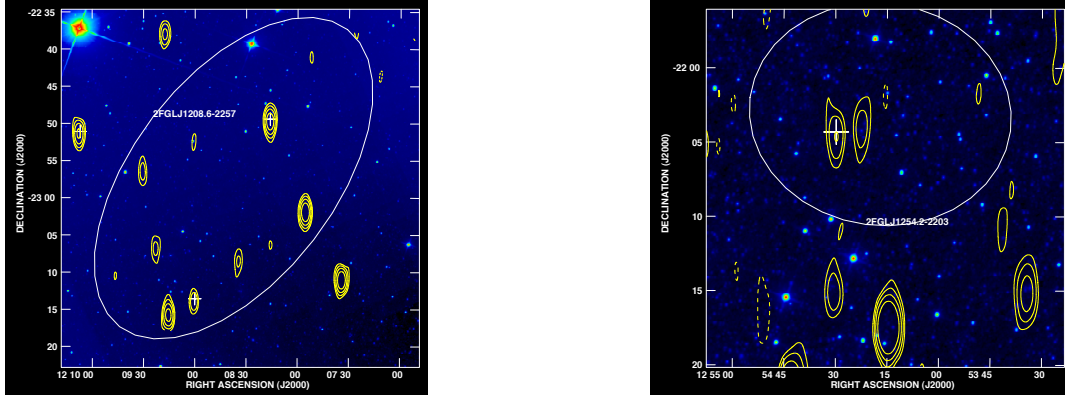


FIG. 1.— Map of the search region around 2FGL J1208–2257 (left panel) and 2FGL J1254.2–2203 (right panel). Color scale background shows the WISE image, contours represent the 352 MHz emission from the WISH, and crosses indicate NVSS sources. The white ellipse is the γ -ray 95% confidence region. In the right panel, our candidate is the left component of the twin NVSS sources (note that the right source is formally not in the WISH catalog).

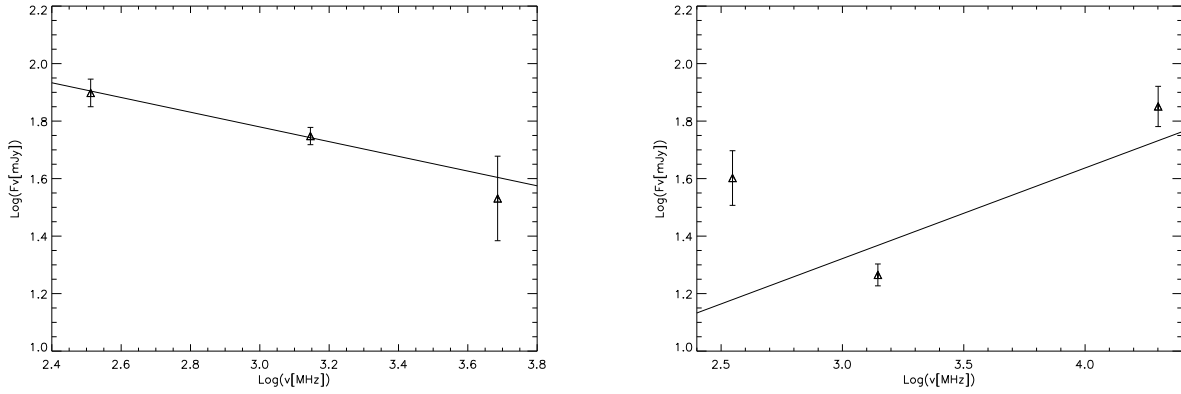


FIG. 2.— Radio spectrum of NVSS J030727+491510 (left panel) and NVSS J125429–220419 (right panel). The solid lines represent the linear regression spectral index, which is clearly a good fit to the data only in the first case.

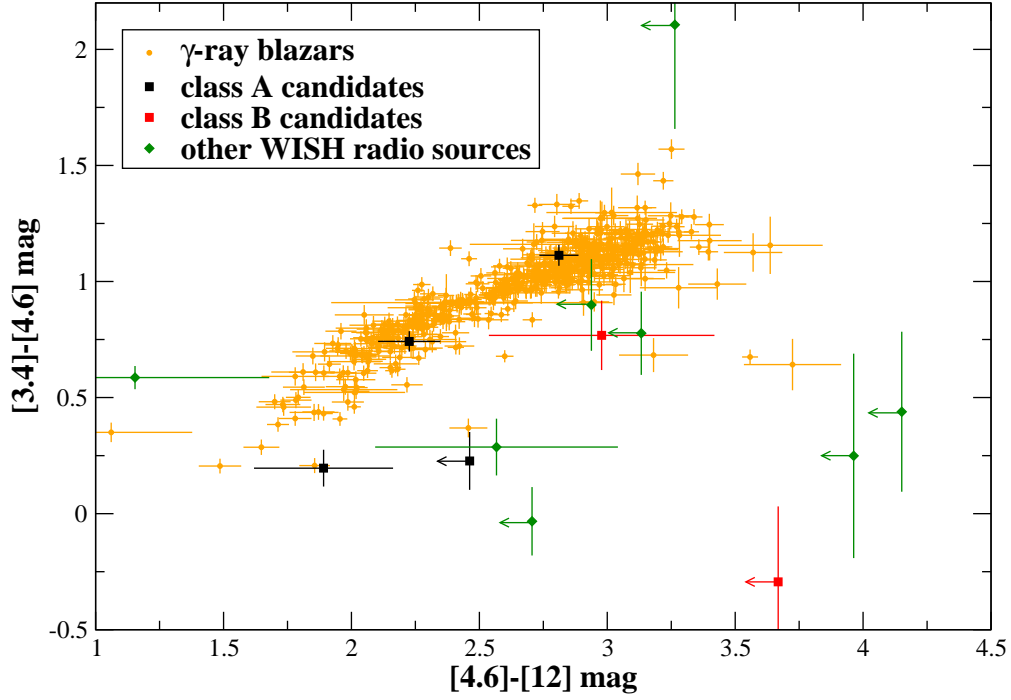


FIG. 3.— The $[3.4] - [4.6] - [12] \mu\text{m}$ color-color plot of all the *WISE* counterparts of the WISH-NVSS sources (green dots) and candidate blazars (black dots: *class A*; red dots: *class B*) in comparison with the blazars that constitute the *WISE* γ -ray strip (orange dots).

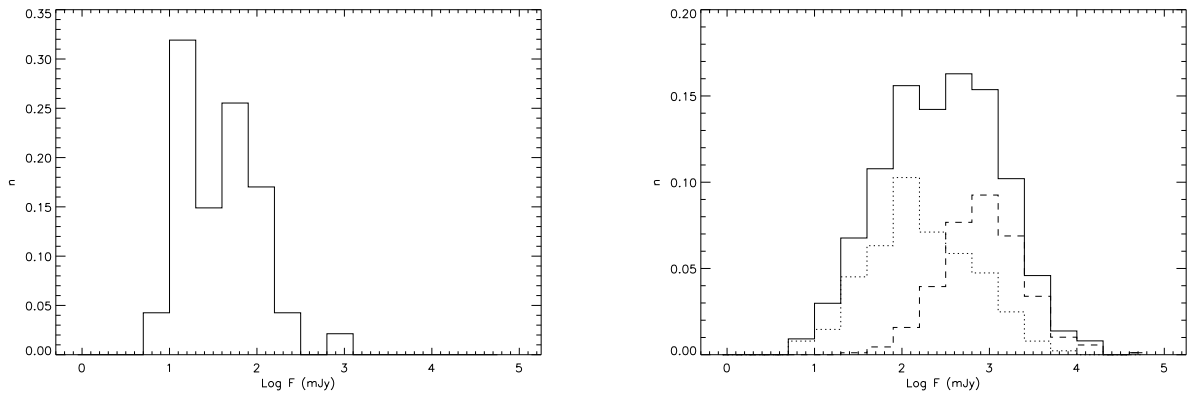


FIG. 4.— Normalized distributions of flux density at 1.4 GHz. Left panel: γ -ray blazar candidates selected among UGS in the WENSS and WISH footprints; right panel: sources in the 2LAC (solid line: all 2 LAC sources, dotted line: BZBs, dashed line: BZQs).

TABLE 1
POSSIBLE BLAZAR-LIKE COUNTERPARTS FOR UGSS IN WISH REGION

2FGL name	WISH name	NVSS name	S_{352} (mJy)	S_{1400} (mJy)	WISE detection	α_{352}^{1400}	Index Class
2FGL J0340.7–2421	WNB 0338.0–2425	NVSS 034011–241602	72 ± 4	23.5 ± 1.1	✓	0.81 ± 0.04	
	WNB 0338.4–2436	NVSS 034033–242712	111 ± 4	82 ± 3	✓	0.22 ± 0.03	A
2FGL J0600.8–1949	WNB 0557.9–1954	NVSS 060003–195446	44 ± 4	12.7 ± 0.6	✓	0.90 ± 0.06	
	WNB 0558.8–1950	NVSS 060100–195049	256 ± 4	96 ± 3	✓	0.71 ± 0.02	
	WNB 0559.4–1948	NVSS 060138–194853	124 ± 4	43.2 ± 1.4		0.76 ± 0.03	
2FGL J1059.9–2051	WNB 1057.1–2037	NVSS 105935–205311	414 ± 8	138 ± 5	✓	0.80 ± 0.02	
	WNB 1057.7–2040	NVSS 110014–205621	737 ± 4	232 ± 7	✓	0.84 ± 0.02	
2FGL J1208.6–2257	WNB 1205.6–2232	NVSS 120816–224925	151 ± 3	66 ± 2		0.60 ± 0.02	B
	WNB 1206.4–2256	NVSS 120900–231335	34 ± 3	28.8 ± 1.0	✓	0.12 ± 0.06	A
	WNB 1207.5–2234	NVSS 121007–225106	96 ± 3	35 ± 1.1		0.73 ± 0.03	
2FGL J1254.2–2203	WNB 1251.8–2148	NVSS 125429–220419	40 ± 4	18.4 ± 0.7		0.56 ± 0.06	A
2FGL J1458.5–2121	WNB 1456.2–2112	NVSS 145904–212357	190 ± 3	70 ± 2	✓	0.73 ± 0.02	
2FGL J1544.5–1126	WNB 1541.4–1115	NVSS 154414–112443	83 ± 3	30.0 ± 1.0		0.74 ± 0.03	
2FGL J1624.2–2124	WNB 1620.5–2058	NVSS 162332–210457	19 ± 3	9.9 ± 0.6		0.47 ± 0.10	A
	WNB 1620.7–2120	NVSS 162345–212716	30 ± 3	19.2 ± 1.5		0.32 ± 0.07	A
	WNB 1621.1–2119	NVSS 162403–212645	175 ± 3	80 ± 3	✓	0.57 ± 0.02	A
	WNB 1623.0–2111	NVSS 162600–211825	105 ± 3	45.2 ± 1.4		0.61 ± 0.03	B
2FGL J1631.0–1050	WNB 1628.0–1045	NVSS 163049–105218	106 ± 5	29.7 ± 1.0		0.92 ± 0.03	
	WNB 1628.7–1037	NVSS 163130–104322	129 ± 5	45.6 ± 1.8		0.75 ± 0.03	
	WNB 1628.8–1044	NVSS 163139–105057	591 ± 5	184 ± 6	✓	0.85 ± 0.02	
2FGL J1646.7–1333	WNB 1644.0–1323	NVSS 164651–132849	447 ± 4	99 ± 3	✓	1.09 ± 0.02	
2FGL J1913.8–1237	WNB 1910.5–1235	NVSS 191320–122949	44 ± 4	14.7 ± 0.6		0.79 ± 0.06	
	WNB 1910.8–1246	NVSS 191339–124120	133 ± 4	39.7 ± 1.3		0.88 ± 0.03	
2FGL J2009.2–1505	WNB 2005.8–1513	NVSS 200838–150500	299 ± 6	105 ± 4		0.76 ± 0.02	
2FGL J2017.5–1618	WNB 2014.9–1627	NVSS 201745–161820	110 ± 3	53.6 ± 1.7		0.52 ± 0.02	A
2FGL J2031.4–1842	WNB 2027.6–1850	NVSS 203030–184033	204 ± 3	92 ± 3		0.58 ± 0.02	B
	WNB 2027.8–1900	NVSS 203044–185033	324 ± 3	134 ± 4	✓	0.64 ± 0.02	B
2FGL J2124.0–1513	WNB 2121.8–1533	NVSS 212438–152017	147 ± 3	40.0 ± 1.3		0.94 ± 0.02	
2FGL J2228.6–1633	WNB 2225.8–1652	NVSS 222830–163643	16 ± 3	20.9 ± 1.1	✓	-0.19 ± 0.10	A
	WNB 2226.0–1641	NVSS 222842–162619	16 ± 3	7.2 ± 0.5		0.58 ± 0.10	A
2FGL J2358.4–1811	WNB 2355.7–1833	NVSS 235820–181621	25 ± 3	9.7 ± 0.6	✓	0.69 ± 0.09	B

TABLE 2
REGRESSION OF RADIO SPECTRAL INDEX WITH GB6 DATA OF WENSS POSSIBLE BLAZAR-LIKE COUNTERPARTS.

NVSS name	Class	$\log S_{325}$ [mJy]	$\log S_{1400}$ [mJy]	$\log S_{4850}$ [mJy]	α_{regr}	α_{325}^{1400}
NVSS J030727+491510	A	1.90 ± 0.05	1.75 ± 0.03	1.53 ± 0.15	0.26 ± 0.08	0.24 ± 0.04
NVSS J033153+630814	A	1.79 ± 0.05	1.63 ± 0.03	1.40 ± 0.16	0.28 ± 0.09	0.26 ± 0.04
NVSS J035309+565431	A	1.98 ± 0.05	1.76 ± 0.03	1.64 ± 0.11	0.32 ± 0.08	0.34 ± 0.04
NVSS J072354+285930	A	1.90 ± 0.06	1.56 ± 0.03	1.49 ± 0.16	0.48 ± 0.10	0.53 ± 0.04
NVSS J150229+555204	A	1.70 ± 0.06	1.54 ± 0.03	1.36 ± 0.17	0.26 ± 0.10	0.25 ± 0.05
NVSS J150147+480335	A	1.43 ± 0.12	1.32 ± 0.03	1.41 ± 0.15	0.06 ± 0.16	0.18 ± 0.08
NVSS J210805+365526	A	1.83 ± 0.05	1.88 ± 0.03	1.83 ± 0.10	-0.04 ± 0.08	-0.08 ± 0.04
NVSS J060102+383828	B	3.261 ± 0.002	2.85 ± 0.03	2.51 ± 0.09	0.65 ± 0.48	0.65 ± 0.02
NVSS J101657+560112	B	2.00 ± 0.04	1.61 ± 0.03	1.79 ± 0.10	0.44 ± 0.06	0.62 ± 0.03

TABLE 3
REGRESSION OF RADIO SPECTRAL INDEX WITH AT20G DATA OF WISH POSSIBLE BLAZAR-LIKE COUNTERPARTS.

NVSS name	Class	$\log S_{352}$ [mJy]	$\log S_{1400}$ [mJy]	$\log S_{20000}$ [mJy]	α_{regr}	α_{352}^{1400}
NVSS J125429-220419	A	1.60 ± 0.10	1.26 ± 0.04	1.85 ± 0.07	-0.31 ± 0.06	0.56 ± 0.06